Cell and Tissue Research (2020) 381:299–308
https://doi.org/10.1007/s00441-020-03196-8

REGULAR ARTICLE

Neuropilin-1 receptor in the rapid and selective estrogen-induced neurovascular remodeling of rat uterus

Analía Richeri[1,2] · Gabriela Vierci[1] · Gaby Fabiana Martínez[1] · María Paula Latorre[1] · Cora Chalar[3] · María Mónica Brauer[1]

Received: 11 March 2019 / Accepted: 27 February 2020 / Published online: 2 April 2020

Abstract

Sympathetic nerves innervate most organs and regulate organ blood flow. Specifically, in the uterus, estradiol (E2) elicits rapid degeneration of sympathetic axons and stimulates the growth of blood vessels. Both physiological remodeling processes, critical for reproduction, have been extensively studied but as independent events and are still not fully understood. Here, we examine the neuropilin-1 (NRP1), a shared receptor for axon guidance and angiogenic factors. Systemic estradiol or vehicle were chronically injected to prepubertal rats and uterine and sympathetic chain sections immunostained for NRP1. Uterine semaphorin-3A mRNA was evaluated by in situ hybridization. Control sympathetic uterine-projecting neurons (1-month-old) expressed NRP1 in their somas but not in their intrauterine terminal axons. Estradiol did not affect NRP1 in the distal ganglia. However, at the entrance of the organ, some sympathetic NRP1-positive nerves were recognized. Vascular NRP1 was confined to intrauterine small-diameter vessels in both hormonal conditions. Although the overall pattern of NRP1-IR was not affected by E2 treatment, a subpopulation of infiltrated eosinophil leukocytes showed immunoreactivity for NRP1. Sema3A transcripts were detected in this cellular type as well. No NRP1-immunoreactive axons nor infiltrated eosinophils were visualized in other estrogenized pelvic organs. Together, these data suggest the involvement of NRP1/Sema3A signaling in the selective E2-induced uterine neurovascular remodeling. Our data support a model whereby NRP1 could coordinate E2-induced uterine neurovascular remodeling, acting as a positive regulator of growth when expressed in vessels and as a negative regulator of growth when expressed on axons.

Keywords Estrogens · Semaphorin-3A · Leukocyte infiltration · Angiogenesis · Neurodegeneration

Introduction

Uterine neural connections represent a simple neural circuit to study the finest mechanisms of remodeling of the nervous system. Neurons innervating the uterus respond to physiological and experimental alterations in systemic levels of estrogens with changes in their terminal axons (Brauer et al. 1995; Chalar et al. 2003; Richeri et al. 2002; Zoubina and Smith 2000). Several studies report that, as a function of the hormonal milieu, cellular, molecular and topographic changes occur in the axonal uterine microenvironment (Brauer and Smith 2015; Chalar et al. 2003; Krizsan-Agbas et al. 2008; Richeri et al. 2010, 2011; Martínez et al. 2016). Among estrogen-induced axon remodeling events that have been reported in rodents and human uteri, the loss of sympathetic axons from the organ is the most remarkable (reviewed in Brauer and Smith 2015). This sympathetic (noradrenergic) denervation of the uterus has been interpreted as an adaptation to promote smooth muscle quiescence and sustained blood flow during gestation.

A striking feature of E2-induced sympathetic denervation of the uterus, not previously attended, is how the terminal nerve fibers are intentionally withdrawn from the organ while blood vessels need to sprout (angiogenesis) within the hypertrophied estrogenized tissue. Indeed, the mechanisms

✉ Analía Richeri
aricheri@iibce.edu.uy

[1] Laboratory of Cell Biology, Instituto de Investigaciones Biológicas Clemente Estable (IIBCE), Avenida Italia 3318, ZP 11600 Montevideo, Uruguay

[2] Department of Experimental Neuropharmacology, Instituto de Investigaciones Biológicas Clemente Estable (IIBCE), Avenida Italia 3318, ZP 11600 Montevideo, Uruguay

[3] Sección Bioquímica, Instituto de Biología, Facultad de Ciencias, UdelaR, Montevideo, Uruguay

through which these two remodeling processes are differentially regulated by E2 in the same organ are not fully understood. Considering that axons and blood vessels share mechanistic principles as they navigate tissues (Carmeliet and Tessier-Lavigne 2005), it is likely that common factors are involved in the coordination of both remodeling processes. Blood vessels influence the trajectories taken by axons to reach their appropriate end organs and in adulthood, they communicate with neurons in order to meet physiological demands (Makita et al. 2008; Long et al. 2009). The balance between guidance molecules and angiogenic factors is coordinated through shared receptors, such as neuropilin-1 (NRP1) (Erskine et al. 2017).

NRP1, originally identified as an adhesion molecule in the nervous system (reviewed in Fujisawa 2004), was subsequently rediscovered as the ligand binding subunit of the semaphorin-3A (Sema3A) receptor in neurons (He and Tessier-Lavigne 1997; Kolodkin et al. 1997) and then in blood vessels as co-receptor of the vascular endothelial growth factor (VEGF) (Hoeben et al. 2004; Plein et al. 2014; Erskine et al. 2017). Notably, both ligands of NRP1, Sema3A (guidance molecule) and VEGF (angiogenic factor) continue to be expressed in adulthood (Brauer and Richeri 2013; Gavazzi 2001; Marzioni et al. 2004; Nangle and Keast 2011; Osol and Mandala 2009) and important implications for neuronal plasticity and nervous system physiology have recently been suggested (Giacobini et al. 2014; Venkova et al. 2014; Vo et al. 2013). We thus hypothesize that NRP1 could be involved in the coordination of neurovascular remodeling processes that occur in the rat uterus in response to estrogens.

Here, we propose to investigate from an integrated point of view two estrogen-dependent remodeling processes, which have been extensively studied as independent events although they occur at the same time, in the same organ. VEGF modulation by estrogen has been studied in the rat uterus related to uterine cyclic vascular remodeling (Cullinan-Bove and Koos 1993; Osol and Mandala 2009; Walter et al. 2010). We previously reported Sema3A upregulation in the prepubertal rat uterus following E2-chronic administration, concomitantly with the angiogenic and neurodegenerative processes that occur within the organ (Richeri et al. 2008). Despite this temporal correlation, the precise site of induction of Sema3A in the estrogenized rat uterus is still unknown. Consistently, Giacobini et al. (2014) demonstrated an endothelium-to-neuron communication mediated by NRP1 signaling in the adult brain. Interestingly, the process is controlled by ovarian-steroid-dependent release of Sema3A, which increases when E2 levels are high, ultimately provoking the extension of GnRH axon terminals that express NRP1 towards the vascular plexus on the day of preovulatory surge (Giacobini et al. 2014). Taken together, these data are consistent with the involvement of NRP1 in the modulation of uterine neurovascular plasticity during reproductive life. However, the expression of NRP1 in uterine-innervating neurons and a possible regulation of its expression by E2 needs to be explored.

In this study, we used the paradigm of chronic exposure of prepubertal female rats to E2 (Brauer et al. 1995; Chalar et al. 2003; Richeri et al. 2002, 2008, 2011) to examine whether uterine-projecting neurons from the paravertebral sympathetic chain (T7-L2) express NRP1 and evaluate the effects of E2. NRP1 levels were assessed using quantitative densitometric immunofluorescence in the retrogradely labeled population of neurons (Cowen et al. 2003; Richeri et al. 2005). Within the uterus, NRP1 immunodetection and Sema3A mRNA localization by in situ hybridization were evaluated.

Materials and methods

Animals

All procedures were carried out in accordance with the Bioethics Committee guidelines, Instituto de Investigaciones Biológicas Clemente Estable (IIBCE) and following the National Institutes of Health guide for the care and use of Laboratory animals (NIH Publications N° 8023, revised 1978) and current ethical regulations under animal experimentation law N° 18.611. Thirty female Wistar rats from the breeding colony held at the IIBCE were used for this study. Animals were sexed at birth, weaned at 3 weeks and maintained under controlled conditions of temperature (22 ± 2 °C) and illumination (12 h light/dark cycles) with water and food provided ad libitum.

Chronic estradiol treatment

Female rats ($n = 14$) were injected subcutaneously (s.c.) with four doses of 10 μg of β-estradiol 17-cypionate (E2) (König, Argentina), or vehicle (peanut oil, Sigma-Aldrich) on days 10, 15, 20 and 25 of postnatal development and killed at 28 days of age (Brauer et al. 1995; Chalar et al. 2003; Richeri et al. 2002, 2011).

Retrograde tracing of uterine-projecting neurons with fluorogold (FG)

Surgical procedures were performed as previously described (Richeri et al. 2005). Briefly, 20-day-old female rats ($n = 16$) were anesthetized with ketamine (90 mg/kg i.p.; Konsol Konig S.A.) and xylazine (10 mg/kg i.p.; Konsol Konig S.A.) and the left uterine horn was exposed through a small dorsal incision. Two to 4 μl of a 4% fluorogold saline solution (FG, Fluorochrome Inc., USA) were injected at the cephalic (tubal) third of the uterine horn. After injection, the muscle and skin were sutured and the animals allowed to recover. On

the 5th, 7th and 9th days following FG injection, the rats were injected (s.c.) with three doses of 20 μg of E2 or vehicle and killed on day 10.

Immunofluorescence

Animals were terminally anesthetized with sodium pentobarbital (Sigma-Aldrich) and transcardially perfused with 25 ml of heparinized (50 IU/ml) 0.9% saline solution followed by 40 ml of freshly prepared 4% paraformaldehyde (PFA, Sigma-Aldrich). The sympathetic paravertebral chains (T7 to L2) ipsilateral to the site of FG injection were dissected. These ganglia contain 65% of the postganglionic sympathetic neurons supplying the cephalic third of the uterine horn (Houdeau et al. 1998). Dissected ganglia were fixed by immersion in 4% PFA for 1.5 h and stored in 12% sucrose in PBS overnight at 4 °C. Ganglia from each animal group were pooled, frozen and completely cryo-sectioned (12 μm). For each set of ganglia, 12–20 slides containing 6–8 sections each were obtained and incubated overnight at room temperature with rabbit anti-neuropilin-1 (anti-NRP1, 1:1000, a generous gift of Prof. DD Ginty, Harvard, USA). The specificity of the immunolabeling was checked by incubating a complementary set of slides with naïve serum. Due to limited amounts of antibody available, no preabsorption experiments were attempted. However, the specificity of this antibody has been previously demonstrated (Kolodkin et al. 1997). The sections were then incubated with goat anti-rabbit IgG conjugated with Alexa-Fluor 568 (1:1600, Thermo Fisher Scientific, USA) for 1.5 h at room temperature and mounted in anti-fade medium.

Uterine horns from prepubertal vehicle- and E2-treated females ($n = 8$) were similarly processed and stained with anti-NRP1 (1:1000); and a subset of sections was co-labeled with rabbit anti-NRP1 and mouse anti-tyrosine hydroxylase (anti-TH 1:200, Thermo Fisher Scientific). Primary antibodies were revealed with goat anti-rabbit IgG conjugated with Alexa-Fluor 568 (1:1600, Thermo Fisher Scientific) and goat anti-mouse IgG conjugated with FITC (1:200, Sigma-Aldrich) respectively. Sections were examined with epifluorescence and laser confocal microscopes (Nikon E800; Olympus FV300) equipped with the appropriate filters and images were captured using 20× or 60× objective lens via CCD digital cameras and acquisition softwares.

After imaging, a subset of estrogenized uterine sections labeled with anti-NRP1 was un-mounted, washed in PBS and stained with hematoxylin/Sirius Red (Direct Red 80, Aldrich Chemical Company, USA), a specific stain for eosinophil leukocytes (Bogomoletz 1980; Richeri et al. 2011).

Assessment of NRP1 immunoreactivity in uterine-projecting neurons

Retrogradely traced uterine-projecting neurons (fluorogold-positive, FG+) showing a nuclear profile were recognized and captured using a × 20 objective lens. Resampling of the same neurons in adjacent sections was avoided by taking images from every fourth section (leaving a gap of 36 μm between sections). Selected neurons were then examined under green light (filter G-2B) to assess the immunofluorescence of NRP1. Digital images were captured within the first 48 h after completing the immunostaining and used for densitometric studies without any contrast or brightness corrections (Cowen and Thrasivoulou 1992). Densitometric assessment of neuronal fluorescence intensity (gray value) was carried out as previously described (Chalar et al. 2003; Richeri et al. 2005). The nuclear and cytoplasmic outlines of neurons were traced interactively and used to generate a mask within which the fluorescence intensity was measured as both the mean optical density per area unit (OD) and integrated optical density per cell profile (IOD = OD× cytoplasmic area) using Image Pro Plus software (Media Cybernetics, USA).

In situ hybridization of Sema3A mRNA

Fresh unfixed uterine horn cryo-sections (12 μm) from vehicle- and estradiol-treated prepubertal animals ($n = 6$) were used for in situ hybridization (ISH) assays (Chalar et al. 2003; Richeri et al. 2011). Sense and antisense digoxigenin-labeled riboprobes were generated from rRsema3a using T7 and Sp6 polymerases (RNA Labelling Kit, Roche, Switzerland). Hybridization was carried out overnight at 50 °C with 50 μl of the hybridization solution containing 2 ng/μl of previously denatured (95 °C, 3 min) digoxigenin-labeled RNA probe. Sections were incubated overnight at 4 °C with 1:2000 alkaline phosphatase (AP)-conjugated anti-digoxigenin antibody (Boehringer Ingelheim, Germany) in blocking solution and color reaction was then developed by incubating with NBT (Nitro Blue Tetrazolium) and BCIP (5-Bromo-1-Chloro-3-Indolyl Phosphate). Sections were fixed in 4% PFA and mounted with 70% glycerol. After imaging, slides were un-mounted, washed in PBS, fixed for 10 min in 4% PFA and stained with Sirius Red (described in "Immunofluorescence" section).

Data analysis

Data were expressed as mean ± S.E.M. Statistical differences between oil- (controls) and E2-treated animals were assessed by Student t test. Values of $P < 0.05$ were considered statistically significant.

Results

NRP1-immunoreactivity in uterine-innervating sympathetic neurons

NRP1-immunoreactivity (NRP1-IR) was visualized in 1-month-old sympathetic neurons (Fig. 1a, c). Uterine-projecting neurons within the sympathetic ganglia were recognized by the presence of yellow-fluorogold (FG) granules in the neuronal cytoplasm (Fig. 1b, d, f, h) and interestingly, were positive for NRP1. No FG-positive neurons with lack of NRP1-IR were found. Neuronal NRP1 positive signal persisted following prepubertal chronic estrogen treatment to rats (Fig. 1e, g). However, levels of fluorescence intensity of NRP1 showed considerable variations among FG-labeled (FG+) neurons, displaying high (arrows, Fig. 1a, g) and low (arrows, Fig. 1c, e) values in ganglia from controls and treated animals, respectively.

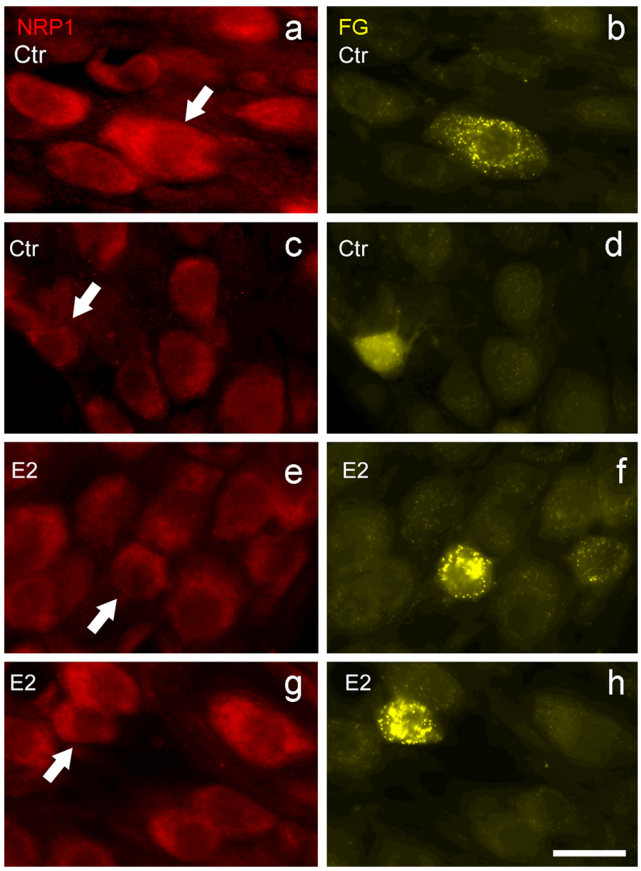

Fig. 1 Representative tissue sections of rat thoraco-lumbar sympathetic chain ganglia showing neurons immunostained for NRP1 (**a**, **c**, **e**, **g**). Expression levels of NRP1 in sympathetic fluorogold-traced (FG) uterine-projecting neurons from controls (Ctr) (**b**, **d**) displaying, respectively, high (**a**, arrow) and low (**c**, arrow) levels of NRP1. FG-positive neurons from estradiol (E2)-treated animals (**f**, **h**) also show marked differences in their levels of NRP1 (**e**, **g**). Calibration bar 25 μm

Effects of estradiol on neuronal NRP1-IR

Densitometric measurements showed no significant changes in the mean optical density (OD) of NRP1 immunofluorescence between control and E2-treated group (Table 1). Frequency histograms for these data revealed that optical density of NRP1 in FG+ control neurons fluctuated between 28 and 135 units and that 59% of these neurons displayed values lower than 70 OD units. Following E2 treatment, no changes in the minimum and maximum values of optical density were detected (Table 1) and a slight shift towards lower values could be visualized due to an increase in the number of neurons with values lower than 70 OD units (controls 59% vs E2 69%).

No significant changes in the mean size of the soma area of uterine-projecting sympathetic neurons were observed following prepubertal chronic estrogen treatment (control 295 ± 34 μm^2 vs estradiol 259 ± 15 μm^2).

NRP1-IR in the uterus of prepubertal vehicle- and estradiol-treated rats

In controls, intense NRP1–1 immunoreactivity was visualized in both the myometrial and endometrial compartments of the uterine horn (Fig. 2). Overall, NRP1-IR was confined to blood vessels (bv, *arrowheads*) and epithelia (*EE*; Fig. 2b). E2 treatment did not alter NRP1-IR distribution in the uterus (Fig. 2c).

Among blood vessels within the myometrium, small-diameter vessels were intensely marked for NRP1 in both hormonal conditions (Fig. 2d–h) and were observed in transverse and longitudinal orientations all along the intramyometrial vascular plexus (IVP) (double *arrowheads and arrowheads,* respectively; Fig. 2d, e). At higher magnifications, vascular NRP1-IR was visualized in the cell membrane (Fig. 2f, g).

Following E2 treatment, eosinophil leukocytes infiltrate the uterus and can be visualized through specific staining with Sirius Red. A subpopulation of NRP1-immunoreactive eosinophil leukocytes that showed variable intensity of labeling

Table 1 Effects of systemic estradiol (E2) on the mean optical density per area unit (OD) of neuropilin-1 (NRP1) fluorescent intensity in fluorogold-positive (FG+) uterine-projecting sympathetic neurons of the rat thoraco-lumbar sympathetic chain. (CTR) oil-treated control group of prepubertal females. Data are expressed as mean ± SEM and were compared by Student *t* test. N = number of neurons

Treatment	*N*	NRP1 OD in FG+ sympathetic neurons	
		Mean OD	Min-max
CTR	178	67 ± 2	28–135
E2	178	64 ± 2	27–144

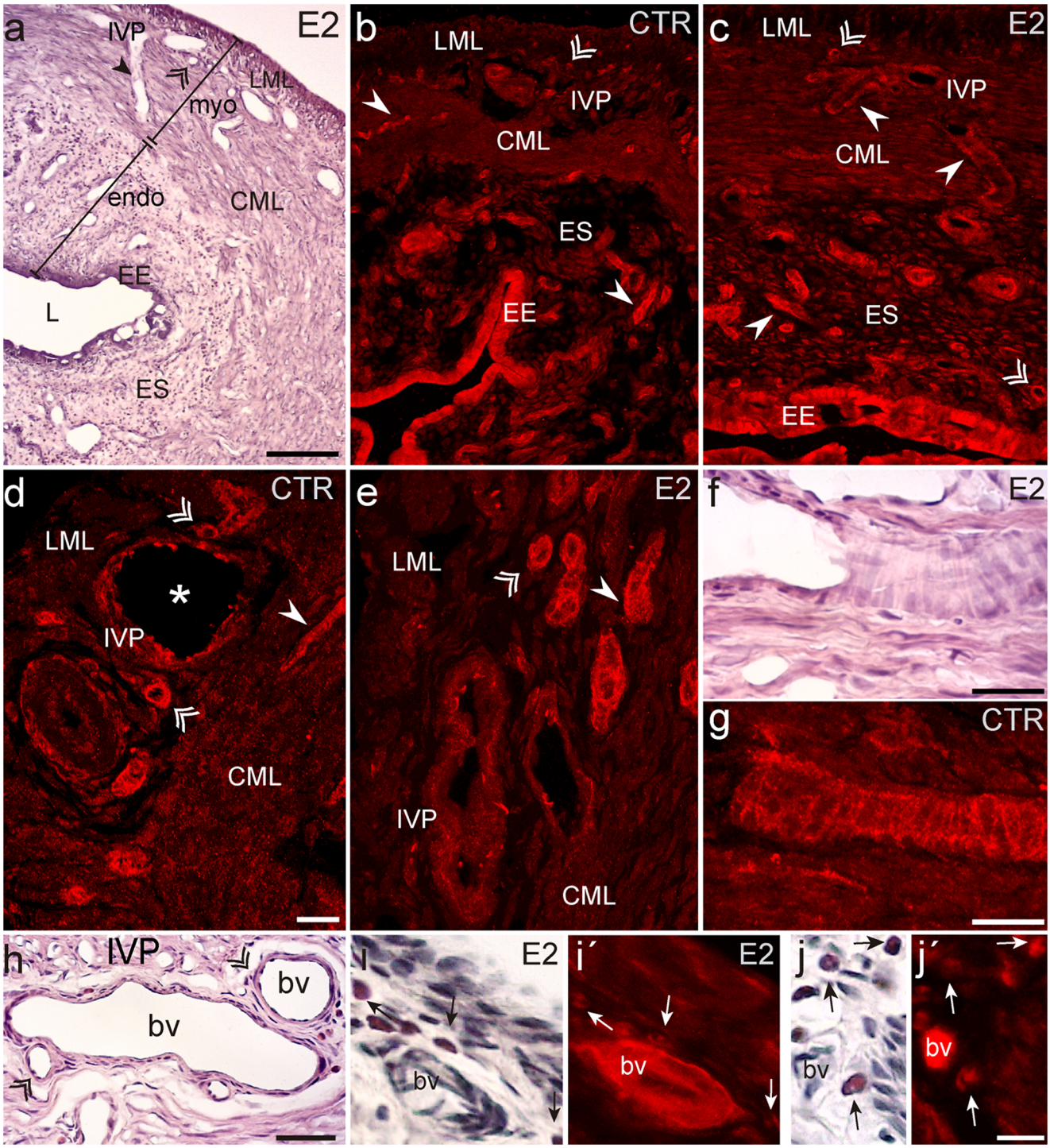

Fig. 2 Panel **a** shows a representative histology of the rat uterine horn (cross-section) stained with hematoxylin and eosin. Panels **b**, **d** and **c**, **e** show neuropilin-1 immunoreactivity in uterine cross-sections of control (CTR) and estradiol (E2)-treated rats, respectively. Note the intense NRP1-IR epithelia and small-diameter vessels. At higher magnifications, the vascular NRP1 signal was visualized in the cell membrane (**f**, **g**). Systemic E2 did not alter NRP1 distribution in the uterus; however, it selectively provoked the infiltration of eosinophil leukocytes, not seen in controls, some of which were immunoreactive for NRP1 (arrows, **i-i′** and **j-j′**). Note that it is the same uterine section has been imaged twice. *Arrows*, eosinophil leukocytes; *arrowheads*, small-diameter blood vessels in transverse (*double-arrowhead*) and longitudinal (*filled-arrowheads*) orientations; *bv*, blood vessel; *CML*, circular myometrial layer; *EE,* endometrial epithelium; *ES*, endometrial stroma; *IVP*, intramyometrial vascular plexus; *L*, lumen; *LML*, longitudinal myometrial layer. Calibration bar in **a**: **a** (660 μm), **b**, **c** (250 μm). Calibration bar in **d**: **d**, **e** (20 μm). Calibration bars: **f** (40 μm), **g** (32 μm), **h** (20 μm). Calibration bar in **j′**: **i-i′** and **j-j′** (8 μm)

was detected surrounding blood vessels in the estrogenized uterus (arrows; Fig. 2i-i′, j-j′).

To further discriminate whether intrauterine sympathetic axons express NRP1, uterine sections from females of both hormonal conditions were co-labeled with anti-NRP1 and anti-tyrosine hydroxylase (TH; a metabolic marker for sympathetic nerve fibers). The myometrium of control females was richly innervated by sympathetic fibers as expected (Fig. 3). Within the myometrial compartment, TH-positive perivascular and myometrial axons were recognized (Fig. 3b, e). None of these intrauterine TH-positive nerve terminals was immunoreactive for NRP1 and thus no signs of co-localization of both antigens were detected (Fig. 3c). Analysis at higher magnification showed that several myometrial sympathetic axons ran freely in the LML (*thin arrows,* Fig. 3d–f). Others were seen to run parallel (*thick filled arrow*) or

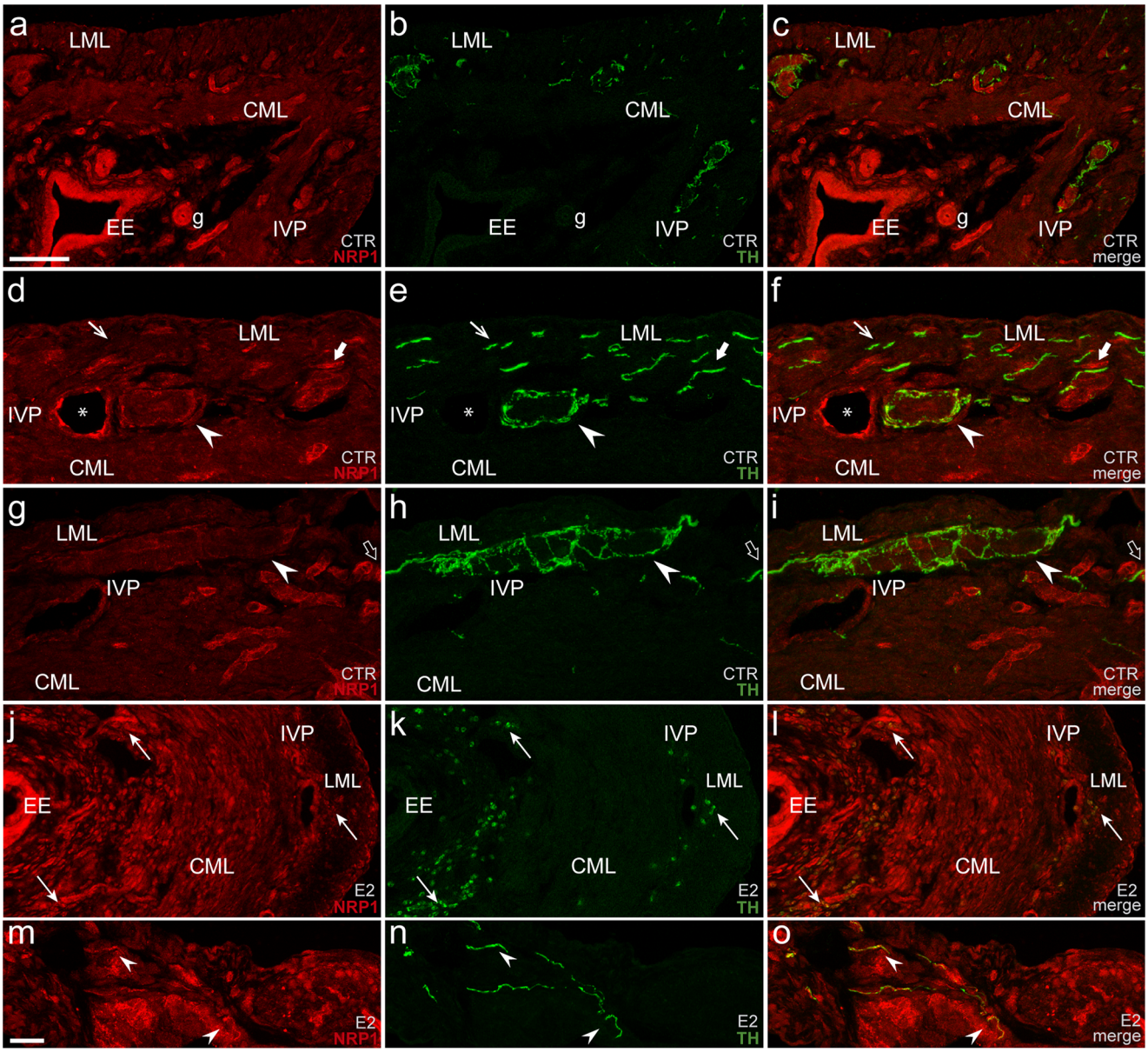

Fig. 3 Representative confocal z-stacks images of control (CTR) (**a**–**i**) and estradiol-treated (E2) (**j**–**o**) uterine horns co-labeled with anti-neuropilin-1 (anti-NRP1, red) and anti-tyrosine hydroxylase (anti-TH, green). In controls, merged images (**c**, **f**, **i**) confirmed that neither perivascular nor myometrial TH-positive axons (**b**, **e**, **h**) were immunoreactive for NRP1. At the end of E2 treatment, no NRP1-immunoreactive (NRP1-IR) nor sympathetic nerve profiles were visualized inside the estrogenized uterus, (**j**–**l**). NRP1-immunoreactive axons (**m**) co-labeled with anti-TH antibody (**n**, **o**) were recognized in the mesometrium following E2 treatment. *Arrows*, eosinophil leukocytes; *arrowheads*, small-diameter blood vessels in transverse (*double-arrowhead*) and longitudinal (*filled-arrowheads*) sections; *bv*, blood vessel; *CML*, circular myometrial layer; *EE,* endometrial epithelium; *IVP*, intramyometrial vascular plexus; *L*, lumen; *LML*, longitudinal myometrial layer. Calibration bar in **a**: **a**–**c**; **j**–**l** (200 μm), **d**–**i** (120 μm). Calibration bar in **m**: **m**–**o** (32 μm)

intermingled (*thick open arrow*) with small-diameter NRP1-positive vessels but without co-localization (Fig. 3d–i).

Following chronic E2 treatment vascular NRP1-IR persisted, as previously mentioned (Figs. 2e, i and 3j) and the expected massive-loss of TH-positive fibers from the myometrium was confirmed (Fig. 3k). No NRP1-immunoreactive axons were detected inside the organ, at the end of E2 treatment (Fig. 3j–l). In the estrogenized mesometrium, TH-positive nerves were occasionally recognized (arrowheads, Fig. 3n). Interestingly, some of these sympathetic nerves were NRP1-immunoreactive and thus, although rarely, co-localized signals were detected at the neuronal level in response to E2 (arrowheads, Fig. 3m–o).

Cellular-specific induction of the NRP1 ligand, Sema3A

In the uterus of prepubertal oil-treated females, Sema3A mRNA was evident in the endometrial stroma, whereas no detectable signal was seen in the epithelium or in endometrial glands (Fig. 4a). No detectable Sema3A transcripts were seen neither in blood vessels (asterisks, Fig. 4a) nor in myometrial cells of the CML.

Following E2 treatment, the Sema3A signal was concentrated in eosinophil leukocytes that infiltrate the endometrium (arrows, Fig. 4b) and myometrium, particularly around blood vessels (asterisks, Fig. 4c, d). Confirmation of the identity of these cells was carried out as before by staining of the in situ hybridized uterine sections with Sirius Red (Fig. 4d-d′, e-e′). In the endometrium, no induction of Sema3A was seen in the endometrial epithelium and glands. No detectable Sema3A transcripts were seen neither in the vascular smooth muscle nor endothelium (Fig. 4d). Positive signal was absent from all regions following hybridization with the sense RNA probe (Fig. 4f).

Discussion

In the present study, we demonstrated that sympathetic uterine-projecting neurons (1-month-old) expressed NRP1 in their somas but not in their axonal connections. Of note, these axons were visualized within the uterine horn along with large-diameter vessels with low NRP1-IR. Systemic E2 treatment had no significant effects on NRP1 in the retrogradely traced uterine-projecting sympathetic cell bodies. However, a small population of sympathetic nerves that persisted at the mesometrium at the end of chronic exposure to estrogen showed NRP1-IR thus suggesting that they might be responsive to the neurorepulsive actions of Sema3A. We identified a population of infiltrating eosinophil leukocytes that distributed around denervated uterine blood vessels and were immunoreactive for NRP1 and synthesized Sema3A mRNA. This finding was exclusively observed in the uterus since no NRP1-immunoreactive eosinophils were visualized in other estrogenized pelvic organs (data not shown). Together, these data suggest the involvement of NRP1/Sema3A signaling in selective E2-induced uterine neurovascular remodeling.

NRP1-immunoreactive neurons that connect to the rat uterus: effects of estrogen

Since estradiol administration is systemic and could be acting directly at the ganglionar level (Papka et al. 2001), we evaluated NRP1 specifically in the sympathetic neurons that connect to the uterus. Sympathetic ganglia contain mixed populations of neurons projecting to the uterus as well as other pelvic targets; thus, uterine-projecting neurons were retrogradely labeled and densitometric analyses of NRP1 fluorescence intensity were conducted. To our knowledge, this was the first study to address E2 modulation of NRP1 in sympathetic neurons. We demonstrated that in vivo 1-month-old uterine-projecting sympathetic neurons express NRP1 and showed that systemic E2 administration does not affect NRP1 fluorescent intensity in the distal sympathetic ganglia.

Uterine vascular vs axonal NRP1 immunoreactivity (NRP1-IR)

Inside the uterus, NRP1 was mainly observed in blood vessels and epithelia. NRP1 expression in blood vessels have been extensively described (Herzog et al. 2001; Kawasaki et al. 1999; Osol and Mandala 2009; Partanen et al. 1999; Pavelock et al. 2001; Plein et al. 2014). Specifically, vascular NRP1 in the adult cyclic rodent uterus and in endothelial cells of the human placenta are consistent with results reported here (Marzioni et al. 2004; Pavelock et al. 2001). Our data also support previous evidence showing no changes in vascular nor epithelial NRP1 expression between control and E2-treated groups of animals (Pavelock et al. 2001; Walter et al. 2010). When expressed in endothelial cells, NRP1 functions as a receptor for VEGF, a key mediator of angiogenesis and vascular permeability (Hoeben et al. 2004; King et al. 2018; Lampropoulou and Ruhrberg 2014). The absence of regulation of NRP1 by E2 does not exclude the possibility that the role of NRP1 in E2-induced uterine remodeling may be locally determined by their ligands (VEGF and/or Sema3A) availability in the estrogenized microenvironment. Consistently, VEGF has been shown to be rapidly induced by estrogen in the rodent uterus (Cullinan-Bove and Koos 1993; Walter et al. 2010). Taken together, these data support the idea that NRP1 expression from uterine vessels may act as a positive regulator of growth. In addition, Sema3A, the other ligand of NRP1, is

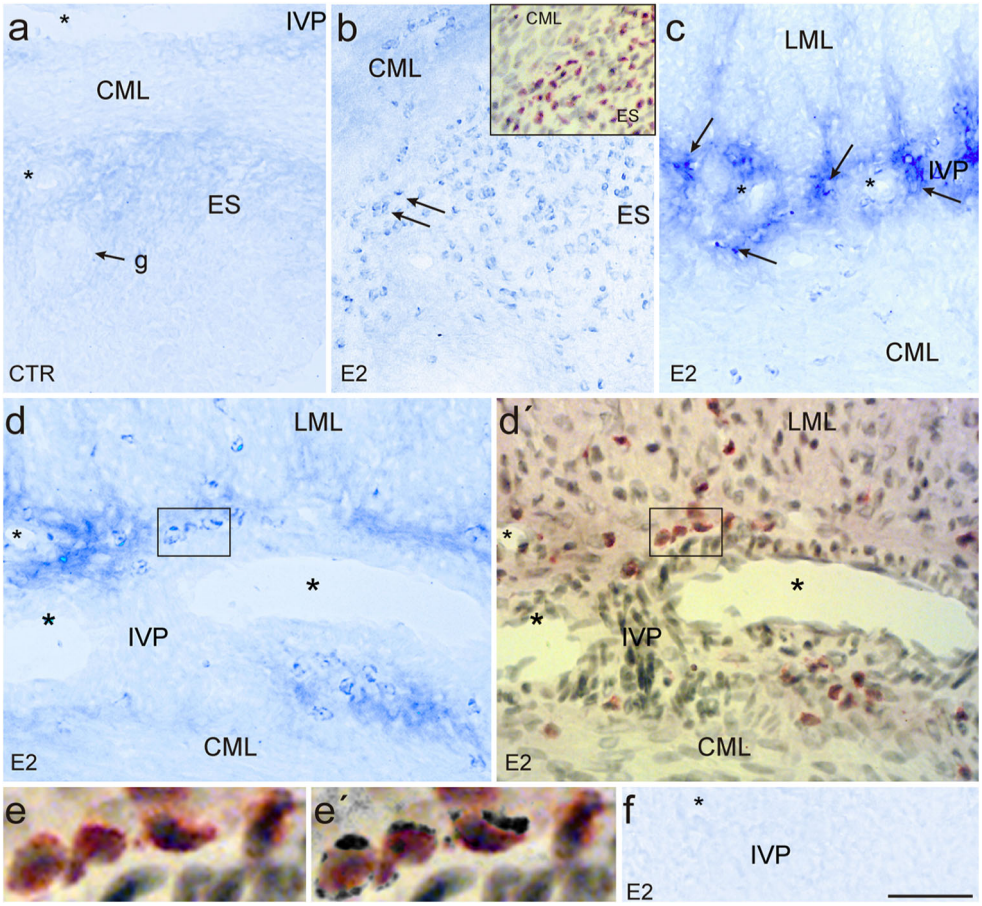

Fig. 4 Representative cross-sections of the uterine horn from prepubertal oil-treated control (CTR) (**a**) and estradiol (E2)-treated rats (**b**–**e**) hybridized with the Sema3A antisense RNA probe. In **f**, a representative uterine section from an E2-treated rat hybridized with a Sema3A sense probe served as negative control. In control uteri, transcripts were visualized in the endometrial stroma (ES) and no vascular (asterisks) Sema3A signal was detected (**a**). Systemic E2 provoked a cellular-specific induction of Sema3A in the endometrium (arrows, **b**) and surrounding blood vessels of the myometrium (**c**, **d**). Staining of hybridized sections with Sirius Red/hematoxylin identified these cells as eosinophil leukocytes (inset in **b** and **d**′). Note that the strong positive signal visualized around blood vessels (asterisks) was not seen in controls. Panels **e**-**e**′ depict a higher magnification of **d**′ (frame), showing the presence of Sema3A transcripts overlapping the cytoplasm of eosinophil leukocytes. CML, circular myometrial layer; ES, endometrial stroma; EE, endometrial epithelium; g, gland; IVP, intramyometrial vascular plexus; LML, longitudinal myometrial layer. Calibration bar: **a**, **b**, **f** (50 μm); **c**-**d**′ (25 μm); **e**, **e**′ (6.5 μm)

upregulated in the prepubertal rat uterus following chronic E2 treatment (Richeri et al. 2008). Our in situ hybridization results (Fig. 4d) demonstrated that Sema3A is not induced in uterine blood vessels as reported in other models (Marko and Damon 2008; Long et al. 2009; Giacobini et al. 2014). This result sheds light on the selective effects of systemic estradiol within the uterus in comparison with other organs.

Finally, here we showed that Sema3A is induced by E2 within the axonal microenvironment and NRP1-positive sympathetic axons were recognized at the mesometrium of E2-treated animals. Sema3A binding to neuronal NRP1 can act as an attractive or a repulsive/degenerative cue depending on the subpopulation of adult neurons (Gavazzi 2001; Giacobini et al. 2014; Nangle and Keast 2011; Venkova et al. 2014; Vo et al. 2013). Specifically, it was shown that Sema3A inhibits growth of adult sympathetic neurons in vitro (Nangle and Keast 2011) and NRP1-IR nerve profiles in the non-pregnant human uterus have been reported thus making these nerves potentially responsive to Sema3A/VEGF during pregnancy (Marzioni et al. 2004; Osol and Mandala 2009). In the present study, no neuronal NRP1-IR was visualized among the densely noradrenergic innervated myometrium of the prepubertal control rats (Fig. 3a–i). Differences in stage of reproductive life or even different immunohistochemical techniques could explain this discrepancy. The possibility that NRP1 levels in myometrial terminal fibers are below the sensitivity threshold for this detection method should not be disregarded.

In sum, together our data are consistent with a model in which NRP1 may have a dual role being a negative regulator of growth when expressed on axons and a positive regulator of growth when expressed on vessels.

E2-induced NRP1 and Sema3A in infiltrating eosinophil leukocytes

Another interesting finding of our study was that the eosinophil leukocytes, a specific leukocyte subpopulation that infiltrates the estrogenized uterus and locate around uterine blood vessels, were loaded with Sema3A transcripts (Fig. 4) and some NRP1-immunoreactive eosinophil leukocytes were also detected (Fig. 2i, j). It has been reported that eosinophil leukocytes also express VEGF (Sastre et al. 2018) as well as another neurorepulsive semaphorin, the Sema3F but not its receptor NRP2 (Richeri et al. 2011). It remains to be addressed whether these signals and receptors are expressed simultaneously in each eosinophil or if there are subpopulations of cells expressing individual signals/receptors or different combinations of these molecules.

Emerging evidence suggests that beyond the axon guidance, particular semaphorin members and their receptors, including Sema3A/NRP1, participate in a broad spectrum of pathophysiological conditions eliciting leukocyte infiltration, monocyte-macrophage retention, platelet hyperreactivity and neovascularization (Hu and Zhu 2018; Marone et al. 2016; Rezaeepoor et al. 2018; Varricchi et al. 2018; Yamazaki et al. 2018). Thus, a possible role of NRP1/Sema3A in the modulation of the selective leukocyte migration to the uterus should be considered. Interestingly, no NRP1 nor Sema3A positive-infiltrated eosinophils were visualized in other estrogenized pelvic organs (data not shown).

Conclusion

Taken together, our results suggest that E2-induced neurovascular remodeling in the uterus could be coordinated by NRP1 in an organ-specific manner and are consistent with a model in which NRP1 expression from vessels may act as a positive regulator of growth and NRP1 on axons may act as a negative regulator of growth. Further functional studies will confirm this dual role of NRP1. E2-induced selective degeneration of sympathetic axons could be triggered by NRP1 signaling via the infiltrated cells. Sema3A could modulate eosinophil leukocyte migration contributing with E2-induced withdrawal of axons (via Sema3F/NRP2) without affecting vascular NRP1 and thus leaving it available for the intrauterine angiogenic factors. Future research will be needed to elucidate the biological function of Sema3A/NRP1 in E2-induced uterine inflammation, angiogenesis and neurodegeneration.

Funding information This study was funded by Fondo Clemente Estable (FCE); Agencia Nacional de Investigación e Innovación (ANII); grant number FCE_3_2016_1_126213 and Programa de Desarrollo de Ciencias Básicas (PEDECIBA-Uruguay).

Compliance with ethical standards

Conflict of interest The authors declare that they have no conflicts of interest.

Ethical approval All procedures were carried out in accordance with the Bioethics Committee guidelines, Instituto de Investigaciones Biológicas Clemente Estable (IIBCE) (Experimental protocols ID: 001/05/2016) and following the National Institutes of Health guide for the care and use of Laboratory animals (NIH Publications N° 8023, revised 1978) and current ethical regulations under animal experimentation law N° 18.611.

References

Bogomoletz W (1980) Advantages de la coloration par le rouge Sirius de l'amyloide et des eosinophiles. Arch Anat Cytol Pathol 28:252–253

Brauer MM, Richeri A (2013) Highlights in basic autonomic neuroscience: semaphorins in the remodeling of autonomic innervation. Auton Neurosci 174:1–4

Brauer MM, Smith PG (2015) Estrogen and female reproductive tract innervation: cellular and molecular mechanisms of autonomic neuroplasticity. Auton Neurosci 187:1–17

Brauer MM, Corbacho A, Burnstock G (1995) Effects of chronic and acute oestrogen treatment on the development of noradrenaline-containing nerves of the rat uterus. Int J Dev Neurosci 13:791–798

Carmeliet P, Tessier-Lavigne M (2005) Common mechanisms of nerve and blood vessel wiring. Nature 436:193–200

Chalar C, Richeri A, Crutcher K, Viettro L, Chávez-Genaro R, Burnstock G, Cowen T, Brauer MM (2003) Oestrogen- and sympathectomy-induced plasticity in developing uterine sensory nerves: the role of NGF. Cell Tissue Res 314:191–205

Cowen T, Thrasivoulou C (1992) A microscopical assay using densitometric application of image analysis to quantify neurotransmitter dynamics. J Neurosci Meth 45:107–116

Cowen T, Woodhoo A, Sullivan C, Jolly R, Crutcher K, Wyatt S, Michael G, Orike N, Gatzinsky K, Thrasivoulou C (2003) Reduced age-related plasticity of neurotrophin receptor expression in sympathetic neurons of the rat. Aging Cell 2:59–69

Cullinan-Bove K, Koos RD (1993) Vascular endothelial growth factor/vascular permeability factor expression in the rat uterus: rapid stimulation by estrogen correlates with estrogen-induced increases in uterine capillary permeability and growth. Endocrinology 133:829–837

Erskine L, François U, Denti L, Joyce A, Tillo M, Bruce F, Vargesson N, Ruhrberg C (2017) VEGF-A and neuropilin 1 (NRP1) shape axon projections in the developing CNS via dual roles in neurons and blood vessels. Development 144:2504–2516

Fujisawa H (2004) Discovery of semaphorin receptors, neuropilin and plexin, and their functions in neural development. J Neurobiol 59:24–33

Gavazzi I (2001) Semaphorin-neuropilin-1 interactions in plasticity and regeneration of adult neurons. Cell Tissue Res 305:275–284

Giacobini P, Parkash J, Campagne C, Messina A, Casoni F, Vanacker C, Langlet F, Hobo B, Cagnoni G, Gallet S, Hanchate NK, Mazur D, Taniguchi M, Mazzone M, Verhaagen J, Ciofi P, Bouret SG, Tamagnone L, Prevot V (2014) Brain endothelial cells control fertility through ovarian-steroid-dependent release of semaphorin 3A. PLoS Biol 12:e1001808

He Z, Tessier-Lavigne M (1997) Neuropilin is a receptor for the axonal chemorepellent semaphorin III. Cell 90:739–751

Herzog Y, Kalcheim C, Kahane N, Reshef R, Neufeld G (2001) Differential expression of neuropilin-1 and neuropilin-2 in arteries and veins. Mech Dev 109:115–119

Hoeben A, Landuyt B, Highley MS, Wildiers H, Van Oosterom AT, De Bruijn EA (2004) Vascular endothelial growth factor and angiogenesis. Pharmacol Rev 56:549–580

Houdeau E, Rousseau A, Meusnier C, Prud'homme M, Rousseau J (1998) Sympathetic innervation of the upper and lower regions of the uterus and cervix in the rat have different origins and routes. J Comp Neurol 399:403–412

Hu S, Zhu L (2018) Semaphorins and their receptors: from axonal guidance to atherosclerosis. Front Physiol 9:1236

Kawasaki T, Kitsukawa T, Bekku Y, Matsuda Y, Sanbo M, Yagi T, Fujisawa H (1999) A requirement for neuropilin-1 in embryonic vessel formation. Development 126:4895–4902

King C, Wirth D, Workman S, Hristova K (2018) Interactions between NRP1 and VEGFR2 molecules in the plasma membrane. Biochim Biophys Acta Biomembr 1860:2118–2125

Kolodkin AL, Levengood DV, Rowe EG, Tai YT, Giger RJ, Ginty DD (1997) Neuropilin is a semaphorin III receptor. Cell 90:753–762

Krizsan-Agbas D, Pedchenko T, Smith PG (2008) Neurotrimin is an estrogen-regulated determinant of peripheral sympathetic innervation. J Neurosci Res 86(14):3086–3095

Lampropoulou A, Ruhrberg C (2014) Neuropilin regulation of angiogenesis. Biochem Soc Trans 42:1623–1628

Long JB, Jay SM, Segal SS, Madri JA (2009) VEGF-A and Semaphorin3A: modulators of vascular sympathetic innervation. Dev Biol 334(1):119–132

Makita T, Sucov HM, Gariepy CE, Yanagisawa M, Ginty DD (2008) Endothelins are vascular-derived axonal guidance cues for developing sympathetic neurons. Nature 452:759–763

Marko SB, Damon DH (2008) VEGF promotes vascular sympathetic innervation. Am J Physiol Heart Circ Physiol 294:H2646–H2652

Marone G, Varricchi G, Loffredo S, Granata F (2016) Mast cells and basophils in inflammatory and tumor angiogenesis and lymphangiogenesis. Eur J Pharmacol 778:146–151

Martínez GF, Bianchimano P, Brauer MM (2016) Estrogen-induced collagen reorientation correlates with sympathetic denervation of the rat myometrium. Auton Neurosci 201:32–39

Marzioni D, Tamagnone L, Capparuccia L, Marchini C, Amici A, Todros T, Bischof P, Neidhart S, Grenningloh G, Castellucci M (2004) Restricted innervation of uterus and placenta during pregnancy: evidence for a role of the repelling signal semaphorin 3A. Dev Dynamics 231:839–848

Nangle MR, Keast JR (2011) Semaphorin 3A inhibits growth of adult sympathetic and parasympathetic neurons via distinct cyclic nucleotide signalling pathways. Br J Pharmacol 162:1083–1095

Osol G, Mandala M (2009) Maternal uterine vascular remodeling during pregnancy. Physiology 24:58–71

Papka RE, Storey-Workley M, Shughrue PJ, Merchenthaler I, Collins JJ, Usip S, Saunders PT, Shupnik M (2001) Estrogen receptor-alpha and beta-immunoreactivity and mRNA in neurons of sensory and autonomic ganglia and spinal cord. Cell Tissue Res 304:193–214

Partanen TA, Makinen T, Arola J, Suda T, Weich HA, Alitalo K (1999) Endothelial growth factor receptors in human fetal heart. Circulation 100:583–586

Pavelock K, Braas K, Ouafik L, Osol G, May V (2001) Differential expression and regulation of the vascular endothelial growth factor receptors neuropilin-1 and neuropilin-2 in rat uterus. Endocrinology 142:613–622

Plein A, Fantin A, Ruhrberg C (2014) Neuropilin regulation of angiogenesis, arteriogenesis, and vascular permeability. Microcirculation 21:315–323

Rezaeepoor M, Ganjalikhani-hakemi M, Shapoori S, Eskandari N, Sharifi M, Etemadifar M, Mansuorian M (2018) Semaphorin-3A as an immune modulator is suppressed by microRNA-145-5p. Cell J 20:113–119

Richeri A, Viettro L, Chavez-Genaro R, Burnstock G, Cowen T, Brauer MM (2002) Effects of infantile/prepubertal chronic estrogen treatment and chemical sympathectomy with guanethidine on developing cholinergic nerves of the rat uterus. J Histo Cyto 50:839–850

Richeri A, Bianchimano P, Marmol NM, Viettro L, Cowen T, Brauer MM (2005) Plasticity in rat uterine sympathetic nerves: the role of TrkA and p75 nerve growth factor receptors. J Anat 207:125–134

Richeri A, Chalar C, Bianchimano P, Greif G, Brauer MM (2008). Estrogen regulation of semaphorin expression in the rat uterus. EMBO Workshop Semaphorin Function and Mechamisms of Action, Abbaye des Vaulx de Cernay, France

Richeri A, Bianchimano P, Crutcher KA, Brauer MM (2010) Reduced sympathetic neurite outgrowth on uterine tissue sections from rats treated with estrogen. Cell Tissue Res 340:287–301

Richeri A, Chalar C, Martínez G, Grief G, Bianchimano P, Brauer MM (2011) Estrogen up-regulation of semaphorin 3F correlates with sympathetic denervation of the rat uterus. Auton Neurosci 164:43–50

Sastre B, Rodrigo-Muñoz JM, García-Sanchez DA, Cañas JA, del Pozo V (2018) Eosinophils: old players in a new game. J Investig Allergol Clin Immunol 28:289–304

Varricchi G, Loffredo S, Galdiero MR, Marone G, Cristinziano L, Granata F, Marone G (2018) Innate effector cells in angiogenesis and lymphangiogenesis. Curr Opin Immunol 53:152–160

Venkova K, Christov A, Kamaluddin Z, Kobalka P, Siddiqui S, Hensley K (2014) Semaphorin 3A signaling through neuropilin-1 is an early trigger for distal axonopathy in the SOD1G93A mouse model of amyotrophic lateral sclerosis. J Neuropathol Exp Neurol 73:702–713

Vo T, Carulli D, Ehlert EM, Kwok JC, Dick G, Mecollari V, Moloney EB, Neufeld G, de Winter F, Fawcett JW, Verhaagen J (2013) The chemorepulsive axon guidance protein semaphorin3A is a constituent of perineuronal nets in the adult rodent brain. Mol Cell Neurosci 56:186–200

Walter LM, Rogers PA, Girling JE (2010) Vascular endothelial growth factor-A isoform and (co) receptor expression are differentially regulated by 17beta-oestradiol in the ovariectomised mouse uterus. Reproduction 140:331–341

Yamazaki T, Li W, Mukouyama Y (2018) Whole-mount confocal microscopy for adult ear skin: a model system to study neuro-vascular branching morphogenesis and immune cell distribution. J Vis Exp. https://doi.org/10.3791/57406

Zoubina EV, Smith PG (2000) Axonal degeneration and regeneration in rat uterus during the estrous cycle. Auton Neurosci 84:176–185